Supplementary Information

Sugar-nucleobase Hydrogen Bonding in the Crystal Structure of Cytidine-5′-monophosphate Nucleotide Cadmium Coordination Complexes

Yaqoot khan,[a] Ismail Ismail,[b] Hongwei Ma,[c] Zhonkui Li,[a] and Hui Li[a]*

[a]Key Laboratory of Cluster Science of Ministry of Education, School of Chemistry and Chemical Engineering, Beijing Institute of Technology, Beijing 100081, P. R. China.

[b]Department of Chemistry and Center for Diagnostics and Therapeutics, Georgia State University, Atlanta, Georgia 30303, United States of America.

[c]Analysis & Testing Center of Beijing Institute of Technology, Beijing 102488, P. R. China.

E-mail: lihui@bit.edu.cn

Tel: 86-10-68912667-602

Fax: 86-10-68914780-804

Table of Contents

1. Crystallographic Data and Structural Information

1.1 Selected bond distances, bond angles, and Hydrogen bonds for complexes 1-5.

Table S1. Selected bond distances (Å) and angles (°) for complex **1**.

Cd(1)–N(2)	2.2961(47)	Cd(1)–O(3)	2.3163(48)
Cd(1)–N(1)	2.3011(50)	Cd(1)–O(5)	2.3434(42)
Cd(1)–O(2)	2.3150(58)	Cd(1)–O(1)	2.4442(44)
P(1)–O(4)	1.5088(47)	P(1)–O(5)	1.5232(46)
P(1)–O(3)	1.5249(49)	P(1)–O(6)	1.6200(42)
N(2)–Cd(1)–N(1)	171.79(22)	O(5)–Cd(1)–O(1)	94.49(17)
N(2)–Cd(1)–O(2)	90.97(24)	O(4)–P(1)–O(5)	113.03(27)
N(1)–Cd(1)–O(2)	97.15(22)	O(4)–P(1)–O(3)	114.76(28)
N(1)–Cd(1)–O(3)	85.54(18)	O(5)–P(1)–O(3)	111.11(26)
O(2)–Cd(1)–O(3)	90.44(17)	O(4)–P(1)–O(6)	102.57(24)
N(2)–Cd(1)–O(5)	92.24(21)	O(5)–P(1)–O(6)	106.97 (24)
N(1)–Cd(1)–O(5)	87.54(17)	O(3)–P(1)–O(6)	107.59(26)
O(2)–Cd(1)–O(5)	83.03(17)	H(12E)–O(12)–H(12B)	110.27
O(3)–Cd(1)–O(5)	169.83(16)	C(13)–O(6)–P(1)	117.47(36)
N(2)–Cd(1)–O(1)	85.08(20)	Cd(1)–O(1)–H(1B)	113.41
N(1)–Cd(1)–O(1)	86.75(18)	Cd(1)–O(1)–H(1D)	113.41
O(2)–Cd(1)–O(1)	175.26(20)	H(1B)–O(1)–H(1D)	110.86
O(3)–Cd(1)–O(1)	92.55(16)	Cd(1)–O(2)–H(2C)	112.85

Symmetric mode: 1-X,1/2+Y, -Z; +X, +Y, -1+Z; 1-X, -1/2+Y, -Z; +X, +Y,1+Z

Table S2. Selected H-bonding distances (Å) and angles (°) for complex **1**.

D–H	d(D–H)	d(H···A)	∠DHA	d(D···A)	A	Symmetry
O(12)–H(12E)	0.850	1.980	173.56	2.827	O5	[-x, y+1/2, -z+1]
O(12)–H(12B)	0.850	2.064	160.27	2.879	O11	[-x+1, y+1/2, -z+1]
O(1)–H(1B)	0.850	2.117	137.05	2.800	O4	[x+1, y, z]
O(1)–H(1D)	0.850	2.214	135.95	2.886	O12	[-x+1, y-1/2, -z+1]
N(5)–H(5B)	0.860	2.344	133.89	3.005	O11	[x-1, y+1, z]
N(5)–H(5C)	0.860	1.993	166.97	2.838	O4	[-x, y+1/2, -z]
O(10)–H(10A)	0.820	2.046	148.63	2.779	N4	[-x, y-1/2, -z+1]
O(9)–H(9A)	0.820	1.810	171.48	2.624	O8	[-x, y-1/2, -z+1]

Table S3. Selected bond distances (Å) and angles (°) for complex **2**.

Cd (1)–O(8)	2.2386(54)	Cd(1)–O(11)	2.3011(54)
Cd (1)–N(1)	2.2727(68)	Cd (1)–O(14)	2.3068(57)
Cd (1)–N(8)	2.2828(64)	Cd (1)–O(6)	2.3308(50)
P(1)–O(1)	1.4857(61)	P(1)–O(4)	1.5106(67)
P(1)–O(6)	1.4924(54)	P(1)–O(16)	1.6110(63)
P(2)–O(8)	1.4762(62)	P(2)–O(13)	1.5367(64)
P(2)–O12	1.4897(68)	P(2)–O(10)	1.5980(68)

O(8)–Cd(1)–N(1)	91.04(24)	O(14)–Cd(1)–O(6)	91.68(21)
O(8)–Cd(1)–N(8)	97.63(25)	O(1)–P(1)–O(6)	112.69(33)
N(1)–Cd(1)–N(8)	169.51(27)	O(1)–P(1)–O(4)	113.13(37)
O(8)–Cd(1)–O(11)	92.41(22)	O(6)–P(1)–O(4)	111.74(36)
N(1)–Cd(1)–O(11)	84.21(26)	O(1)–P(1)–O(16)	102.50(36)
N(8)–Cd(1)–O(11)	89.51(28)	O(6)–P(1)–O(16)	107.58(34)
O(8)–Cd(1)–O(14)	173.22(23)	O(4)–P(1)–O(16)	108.57(40)
N(1)–Cd(1)–O(14)	84.82(25)	O(8)–P(2)–O(12)	118.03(38)
N(8)–Cd(1)–O(14)	87.08(25)	O(8)–P(2)–O(13)	112.26(34)
O(11)–Cd(1)–O(14)	92.51(22)	O(12)–P(2)–O(13)	106.54(40)
O(8)–Cd(1)–O(6)	83.11(20)	O(8)–P(2)–O(10)	103.98(34)
N(1)–Cd(1)–O(6)	92.36(23)	O(12)–P(2)–O(10)	110.48(37)
N(8)–Cd(1)–O(6)	94.53(25)	O(13)–P(2)–O(10)	104.83(39)
O(11)–Cd(1)–O(6)	174.32(24)		

Symmetric mode: -1+X, +Y, +Z; 1+X, +Y, +Z

Table S4. Selected H-bonding distances (Å) and angles (°) for complex **2**.

D–H	d(D–H)	d(H···A)	∠DHA	d(D···A)	A	Symmetry
O(14)–H(14A)	0.85	1.91	153.6	2.697	O1	
O(14)–H(14B)	0.85	2.08	137.7	2.773	O17	[-x, y+1/2, -z+1/2]
O(20)–H(20)	0.82	2.08	142.3	2.775	O4	[x+1/2, -y+3/2, -z+1]
O(11)–H(11A)	0.85	1.85	151.9	2.629	O1	[-x, y-1/2, -z+1/2]
O(11)–H(11B)	0.85	2.02	173.5	2.865	O2	
N(2)–H(2)	0.78	2.11	168.0	2.877	N3	[-x+1, y-1/2, -z+1/2]
N(5)–H(5B)	0.86	2.13	168.9	2.976	O4	[-x, y-1/2, -z+1/2]
N(5)–H(5A)	0.86	1.97	173.9	2.822	O3	[-x+1, y-1/2, -z+1/2]
O(15)–H(15)	0.82	1.84	158.5	2.621	O9	
N(7)–H(7A)	0.86	2.12	171.7	2.970	O7	[-x+1, y+1/2, -z+1/2]
O(17)–H(17A)	0.85	1.87	148.2	2.632	O12	
O(9)–H(9B)	0.85	1.88	158.9	2.690	O4	[x+1/2, -y+3/2, -z+1]

Table S5. Selected bond distances (Å) and angles (°) for complex **3**.

Cd(1)–O(1)	2.250(3)	Cd(1)–N(4)	2.344(3)
Cd(1)–O(2)	2.234(3)	P(1)–O(5)	1.516(2)
Cd(1)–O(3)	2.300(3)	P(1)–O(6)	1.514(3)
Cd(1)–O(4)	2.339(3)	P(1)–O(7)	1.615(2)
Cd(1)–N(1)	2.330(3)	P(1)–O(8)	1.514(3)
O(1)–Cd(1)–O(3)	91.79(9)	O(3)–Cd(1)–N(4)	86.47(12)
O(1)–Cd(1)–O(4)	176.04(11)	O(4)–Cd(1)–N(4)	87.38(11)
O(1)–Cd(1)–N(1)	87.50(11)	N(1)–Cd(1)–O(4)	92.11(10)
O(1)–Cd(1)–N(4)	92.99(11)	N(1)–Cd(1)–N(4)	179.47(11)
O(2)–Cd(1)–O(1)	93.12(10)	O(5)–P(1)–O(7)	102.93(13)
O(2)–Cd(1)–O(3)	173.89(10)	O(6)–P(1)–O(5)	113.56(15)
O(2)–Cd(1)–O(4)	90.83(10)	O(6)–P(1)–O(7)	106.85(14)
O(2)–Cd(1)–N(1)	90.54(13)	O(6)–P(1)–O(8)	112.41(17)
O(2)–Cd(1)–N(4)	89.63(13)	O(8)–P(1)–O(5)	112.46(16)
O(3)–Cd(1)–O(4)	84.30(11)	O(8)–P(1)–O(7)	107.84(16)
O(3)–Cd(1)–N(1)	93.32(12)		

Symmetric mode: +X, +Y, -1+Z; +X, +Y,1+Z

Table S6. Selected H-bonding distances (Å) and angles (°) for complex **3**.

D–H	d(D–H)	d(H···A)	∠DHA	d(D···A)	A	Symmetry
O(1)–H(1A)	0.85	1.82	171.2	2.664	O5	
O(1)–H(1B)	0.86	2.01	135.0	2.688	O6	[2-X,1/2+Y,1-Z]
O(2)–H(2A)	0.85	1.80	164.1	2.623	O15	[1-X, -1/2+Y,1-Z]
O(2)–H(2B)	0.85	1.89	159.1	2.698	O6	
O(3)–H(3A)	0.89	1.72	162.2	2.580	O8	[2-X,1/2+Y,1-Z]
O(3)–H(3B)	0.89	1.87	161.7	2.728	O14	[1-X,1/2+Y,1-Z]
O(4)–H(4B)	0.88	1.81	157.5	2.646	O8	[-1+X, +Y, +Z]
O(10)–H(10A)	0.82	1.79	164.5	2.585	O12	[2-X, -1/2+Y,2-Z]
O(11)–H(11)	0.82	2.06	168.1	2.863	N6	[2-X, -1/2+Y,2-Z]
N(7)–H(7B)	0.86	1.97	168.2	2.818	O5	[-X,1/2+Y,1-Z]
O(13)–H(13A)	0.85	1.97	166.8	2.805	O10	
O(13)–H(13B)	0.85	2.00	172.5	2.846	O6	
O(14)–H(14C)	0.85	1.97	150.8	2.746	O13	
O(15)–H(15A)	0.85	2.01	158.0	2.819	O5	[-1+X, +Y, +Z]

Table S7. Selected bond distances (Å) and angles (°) for complex **4**.

Cd(1)–O(1)	2.245(3)	P(1)–O(5)	1.563(4)
Cd(1)–O(2)	2.232(3)	P(1)–O(6)	1.491(4)
Cd(1)–O(3)	2.319(3)	P(1)–O(7)	1.598(4)
Cd(1)–O(4)	2.299(3)	P(2)–O(2)	1.520(3)
Cd(1)–N(1)	2.315(3)	P(2)–O(11)	1.496(3)
Cd(1)–N(2)	2.325(4)	P(2)–O(12)	1.516(4)
P(1)–O(1)	1.495(3)	P(2)–O(13)	1.607(3)
O(1)–Cd(1)–O(2)	84.41(11)	N(2)–Cd(1)–O(2)	92.16(13)
O(1)–Cd(1)–O(3)	174.72(12)	O(1)–P(1)–O(5)	112.00(19)
O(1)–Cd(1)–O(4)	92.29(12)	O(1)–P(1)–O(7)	104.44(19)
O(1)–Cd(1)–N(1)	96.34(14)	O(5)–P(1)–O(7)	105.6(2)
O(1)–Cd(1)–N(2)	91.19(13)	O(6)–P(1)–O(1)	117.6(2)
O(3)–Cd(1)–O(2)	91.04(11)	O(6)–P(1)–O(5)	107.1(2)
O(3)–Cd(1)–N(2)	86.31(14)	O(6)–P(1)–O(7)	109.5(2)
O(4)–Cd(1)–O(2)	176.20(13)	O(2)–P(2)–O(13)	107.36(18)
O(4)–Cd(1)–O(3)	92.16(12)	O(11)–P(2)–O(2)	113.20(18)
O(4)–Cd(1)–N(1)	89.51(15)	O(11)–P(2)–O(12)	113.0(2)
O(4)–Cd(1)–N(2)	86.00(14)	O(11)–P(2)–O(13)	102.9(2)
N(1)–Cd(1)–O(2)	92.74(14)	O(12)–P(2)–O(2)	111.6(2)
N(1)–Cd(1)–O(3)	86.52(14)	O(12)–P(2)–O(13)	108.1(2)
N(1)–Cd(1)–N(2)	171.39(14)		

Symmetric mode: 1+X, +Y, +Z; -1+X, +Y, +Z

Table S8. Selected H-bonding distances (Å) and angles (°) for complex **4**.

D–H	d(D–H)	d(H···A)	∠DHA	d(D···A)	A	Symmetry
O(3)–H(3A)	1.00	1.82	159.2	2.775	O20	
O(4)–H(4A)	0.96	1.78	150.7	2.661	O11	[2-X,1/2+Y,1/2-Z]
O(4)–H(4B)	0.96	1.99	146.3	2.845	O19	
O(5)–H(5)	0.82	1.74	175.8	2.558	O2	
O(9)–H(9)	0.82	1.88	154.3	2.641	O17	
O(15)–H(15)	0.82	2.10	140.1	2.779	O12	[-1/2+X,1/2-Y,1-Z]
N(6)–H(6)	0.86	2.00	173.9	2.856	N9	[1-X,1/2+Y,1/2-Z]
N(7)–H(7A)	0.86	1.92	175.6	2.779	O16	[1-X,1/2+Y,1/2-Z]
O(17)–H(17A)	0.85	1.90	164.5	2.725	O12	[-1/2+X,1/2-Y,1-Z]
O(17)–H(17B)	0.85	2.00	167.1	2.836	O18	
O(19)–H(19A)	0.85	2.00	170.1	2.841	O20	
O(20)–H(20A)	0.85	1.99	161.9	2.812	O9	[3/2-X,1-Y, -1/2+Z]
O(20)–H(20B)	0.85	1.85	164.3	2.680	O6	[3/2-X,1-Y, -1/2+Z]

Table S9. Selected bond distances (Å) and angles (°) for complex **5**.

Cd(1)–O(1)	2.313(2)	P(1)–O(4)	1.536(18)
Cd(1)–O(2)	2.331(2)	P(1)–O(5)	1.519(2)
Cd(1)–O(3)	2.357(2)	P(1)–O(6)	1.526(18)
Cd(1)–O(4)	2.274(19)	P(1)–O(7)	1.623(19)
Cd(1)–N(1)	2.365(2)		
Cd(1)–N(2)	2.362(2)		

O(1)–Cd(1)–O(2)	89.10(9)	O(2)–Cd(1)–N(1)	89.57(8)
O(1)–Cd(1)–O(3)	173.18(7)	O(1)–Cd(1)–N(2)	88.12(7)
O(2)–Cd(1)–O(3)	85.26(8)	O(3)–Cd(1)–N(1)	86.68(9)
O(4)–Cd(1)–O(1)	93.67(8)	O(3)–Cd(1)–N(2)	96.47(8)
O(4)–Cd(1)–O(2)	174.98(7)	O(4)–Cd(1)–N(1)	94.64(7)
O(4)–Cd(1)–O(2)	91.04(11)	O(4)–Cd(1)–N(2)	87.84(7)
O(3)–Cd(1)–N(2)	86.31(14)	O(4)–P(1)–O(7)	107.18(9)
O(4)–Cd(1)–O(2)	176.20(13)	O(5)–P(1)–O(4)	114.72(11)
O(4)–Cd(1)–O(3)	92.23(8)	O(5)–P(1)–O(6)	112.10(11)
O(1)–Cd(1)–N(1)	89.44(8)	O(5)–P(1)–O(7)	103.26(11)
O(1)–Cd(1)–N(2)	87.16(8)	O(6)–P(1)–O(4)	111.09(10)
N(2)–Cd(1)–N(1)	175.92(7)	O(6)–P(1)–O(7)	107.85(10)

Table S10. Selected H-bonding distances (Å) and angles (°) for complex **5**.

D–H	d(D–H)	d(H···A)	∠DHA	d(D···A)	A	Symmetry
O(1)–H(1A)	0.85	1.87	176.6	2.721	O6	[1+X, +Y, +Z]
O(1)–H(1B)	0.85	1.88	167.7	2.721	O12	[3-X, -1/2+Y,2-Z]
O(2)–H(2A)	0.85	1.91	167.7	2.748	O6	[3-X,1/2+Y,2-Z]
O(2)–H(2B)	0.85	2.05	169.1	2.893	O5	[1+X, +Y,+Z]
O(3)–H(3A)	0.85	2.05	150.4	2.823	O5	
O(3)–H(3B)	0.85	2.17	136.1	2.849	O4	[3-X,1/2+Y,2-Z]
O(9)–H(9A)	0.82	1.88	150.9	2.627	O11	[2-X, -1/2+Y,3-Z]
O(10)–H(10)	0.82	2.08	166.8	2.886	N4	[2-X, -1/2+Y,3-Z]
O(12)–H(12A)	0.85	1.86	160.0	2.671	O5	
O(12)–H(12B)	0.88	2.01	150.7	2.806	O13	

Table S11. The metal···metal distances and dihedral angles in complexes **1-5**.

	1	**2**	**3**	**4**	**5**
metal···metal distances (Å)	13.8950(31)	13.8130(51)	13.6250(19)	13.5898(15)	14.109(8)
dihedral angles a (°)	62.3(3)	23.8(4)	25.80(17)	22.4(2)	52.18(11)

Table S12. The intra- and inter-chain π-π stacking interactions and the conformation of ribose for complexes **1-5**.

	1	**2**	**3**	**4**	**5**
π–π stacking[a] (Å)	–	3.732 3.969	–	3.736 3.881	– –
π–π stacking[b] (Å)	3.757	3.683 3.781	3.687	3.814 3.928	– –
Conformation of ribose	*T*	*T*	*T*	*T*	*T*
Dimension	2D	1D	1D	1D	1D

[a] Intra-chain π-π stacking interactions (Å).
[b] Inter-chain π-π stacking interactions (Å).

2. Supporting information of Complex 1
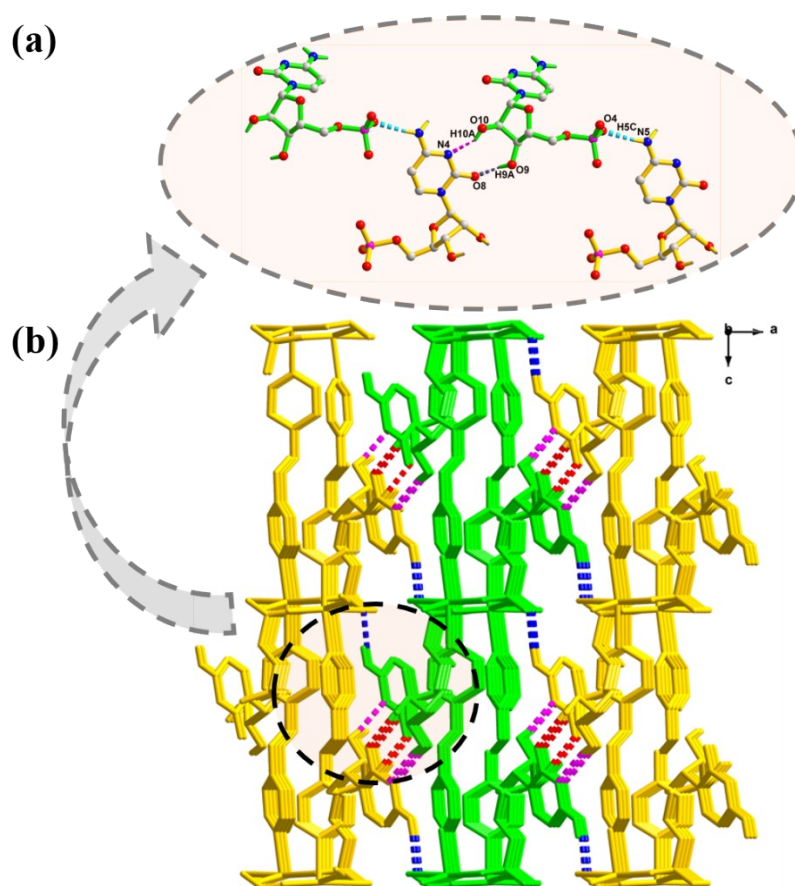
Figure S1. (a) The sugar-nucleobase hydrogen bond pairs between CMP ligands as well as phosphate. 3D supramolecular framework based on hydrogen bonding viewed down from the *b*-axis.
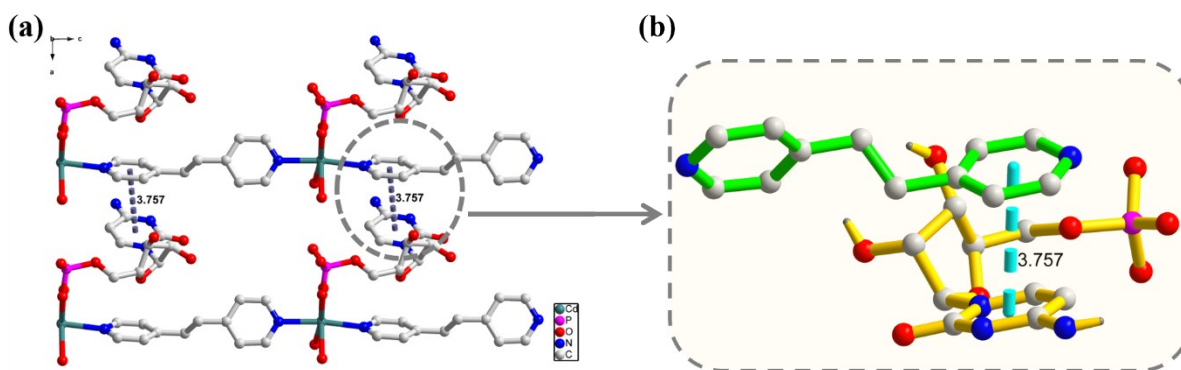
Figure S2. 2D structure based on π–π stacking interaction viewed down from the *b*-axis.
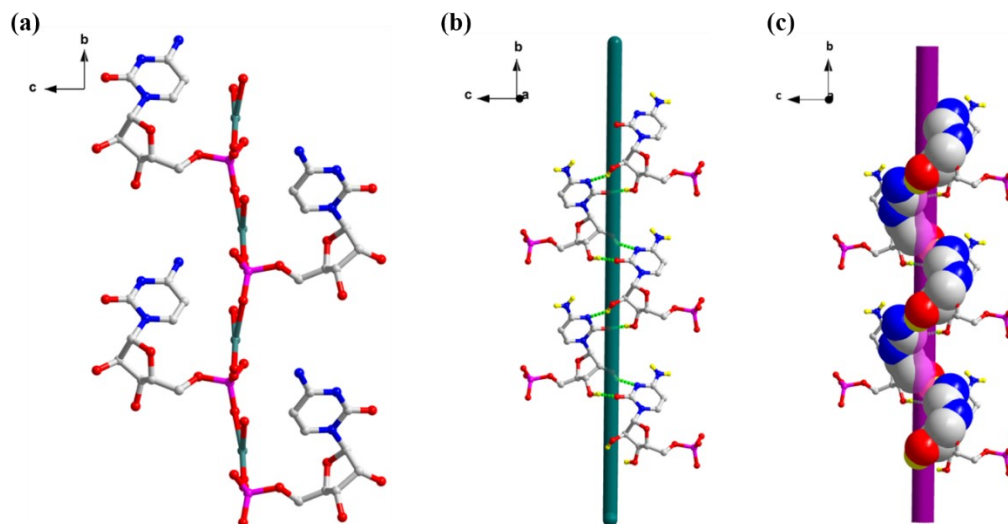
Figure S3. (a) 2D coordination polymer formed by nucleotide ligands connecting the cadmium–phosphate chains (green atom shows the six-coordinate cadmium ions). 1,2-bis(4-pyridyl) ethane ligands are omitted for clarity. (b) and (c) Supramolecular helix formed by hydrogen bonding between sugar-nucleobase interaction of **1**.
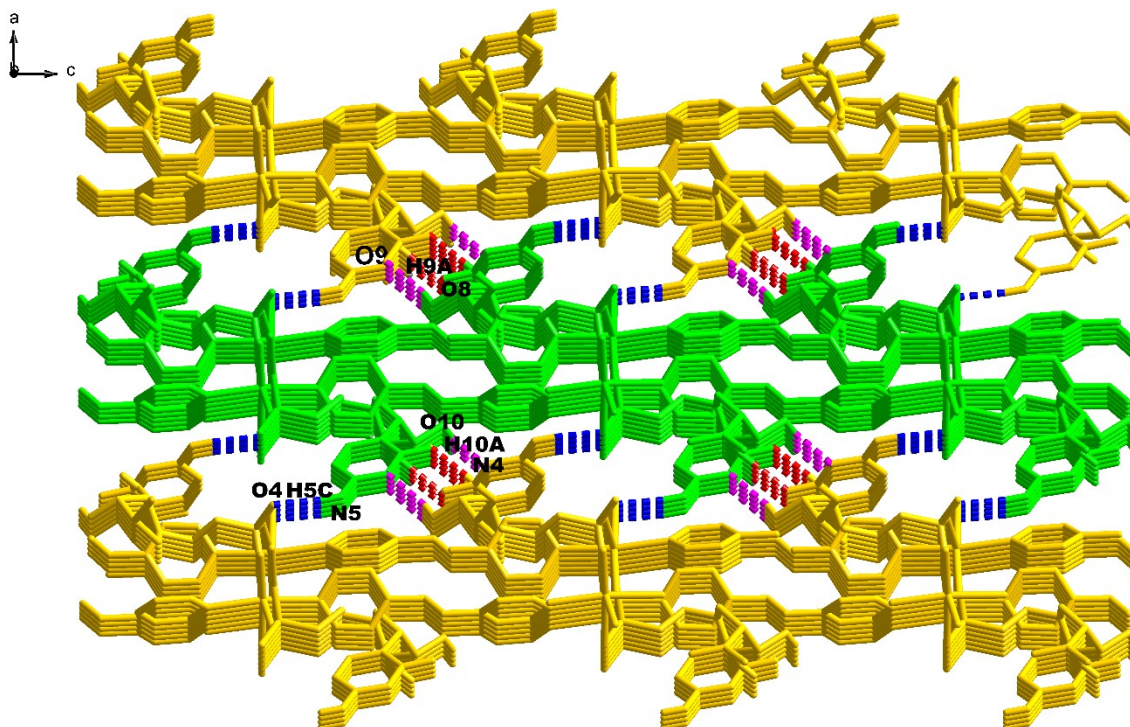
Figure S4. 3D supramolecular framework based on hydrogen bonding viewed down from the *b*-axis. The hydrogen bonding of the sugar-ring hydroxyl group to the carbonyl oxygen atom and the imine nitrogen atom of the base (red and pink dashed lines, N4···O10-H10A, 2.046 Å, O9–H9A···O8, 1.810 Å). H-bond between phosphate oxygen and pyrimidine base (blue dashed lines, N5–H5C···O4, 1.994 Å).

(a)

(b)

62.3°   Dihedral Angle

(c)
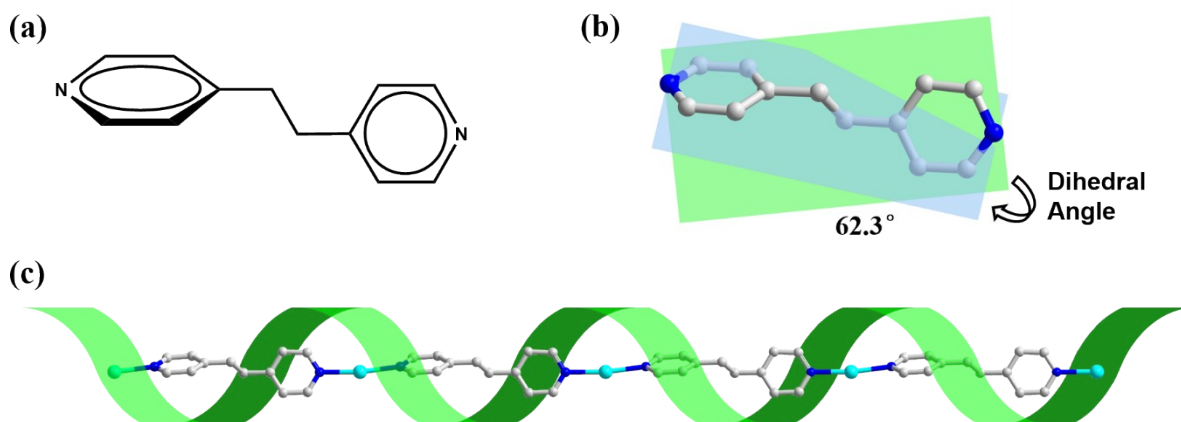
Figure S5. The dihedral angle of the plane formed by the methylene and pyridine ring in bpa ligand complex **1**.

(a)

(b)
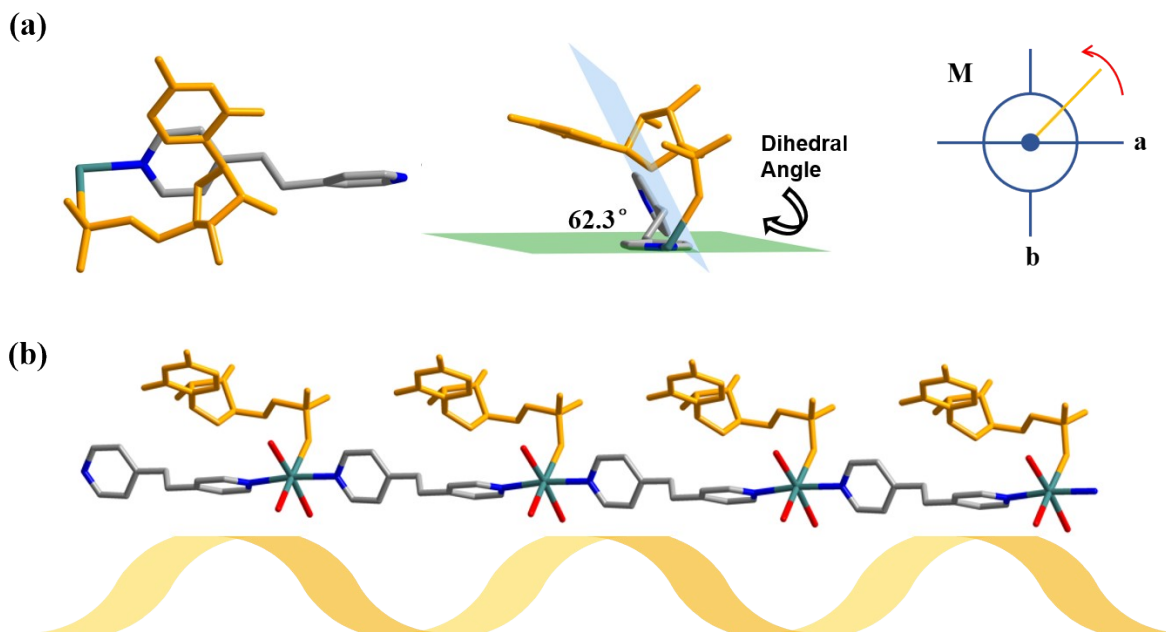
Figure S6. (a) The dihedral angle of bpa in complex **1**; the counter-clockwise orientated nucleotide ligand inducing *M*-supramolecular chirality. (c) EAC chirality in complex **1** generated from M-L coordination and inducement of chiral nucleotides.

3. Supporting information of Complex 2
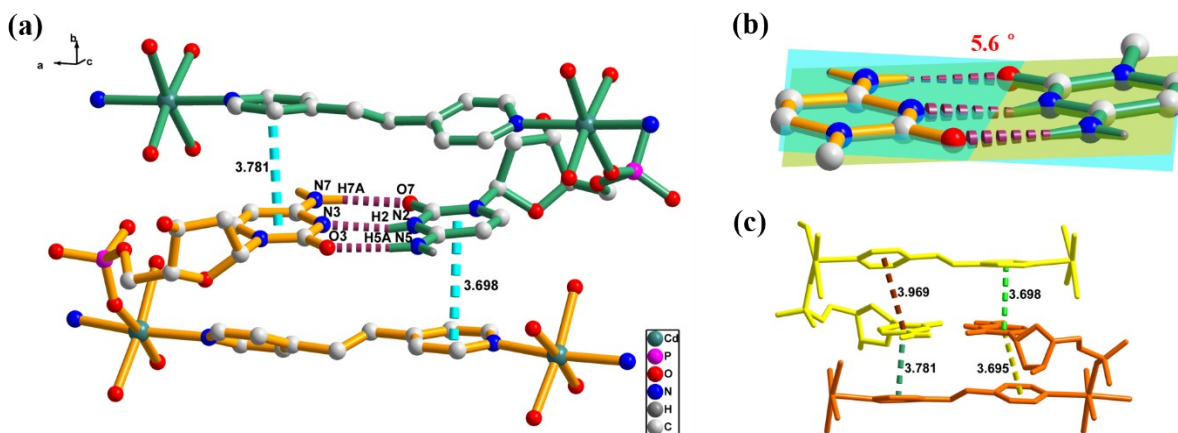
Figure S7. (a) i-motif and π–π stacking interactions and complementary H-bonding between nucleobases. (b) i-motif angle in complex **2**, (c) the i-motif further stabilized by H-bonding and π–π stacking interactions.
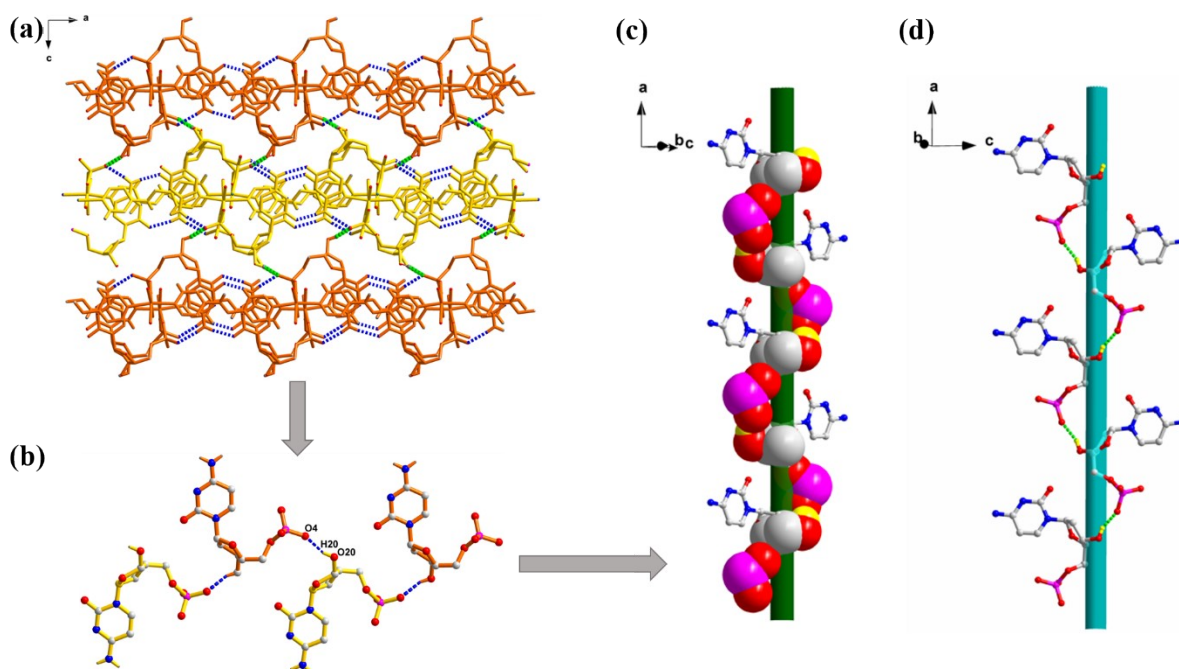
Figure S8. (a) The 3D supramolecular structure of **2** assembled by O20–H20···O4 representing in green dotted, H-bonding between the phosphate group and O-H donors of hydroxy of pentose (O20–H20···O4 2.08 Å, 2.77 Å, 142°). (b) H-bonding between pyrimidine base and the phosphate group in complex **2**. (c) and (d) Supramolecular helix based on hydrogen bond forming between the oxygen of phosphate group and hydroxy group of pentose (O20–H20···O4 2.08 Å, 2.77 Å, 142°) of **2**.
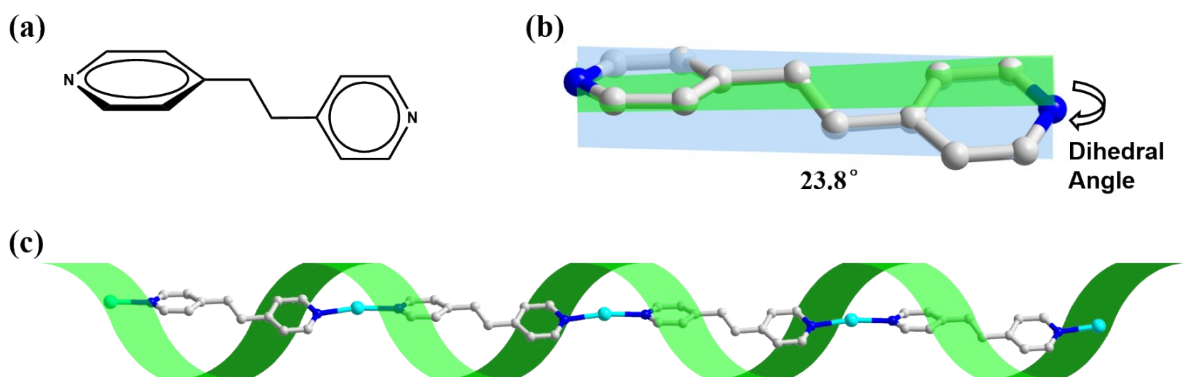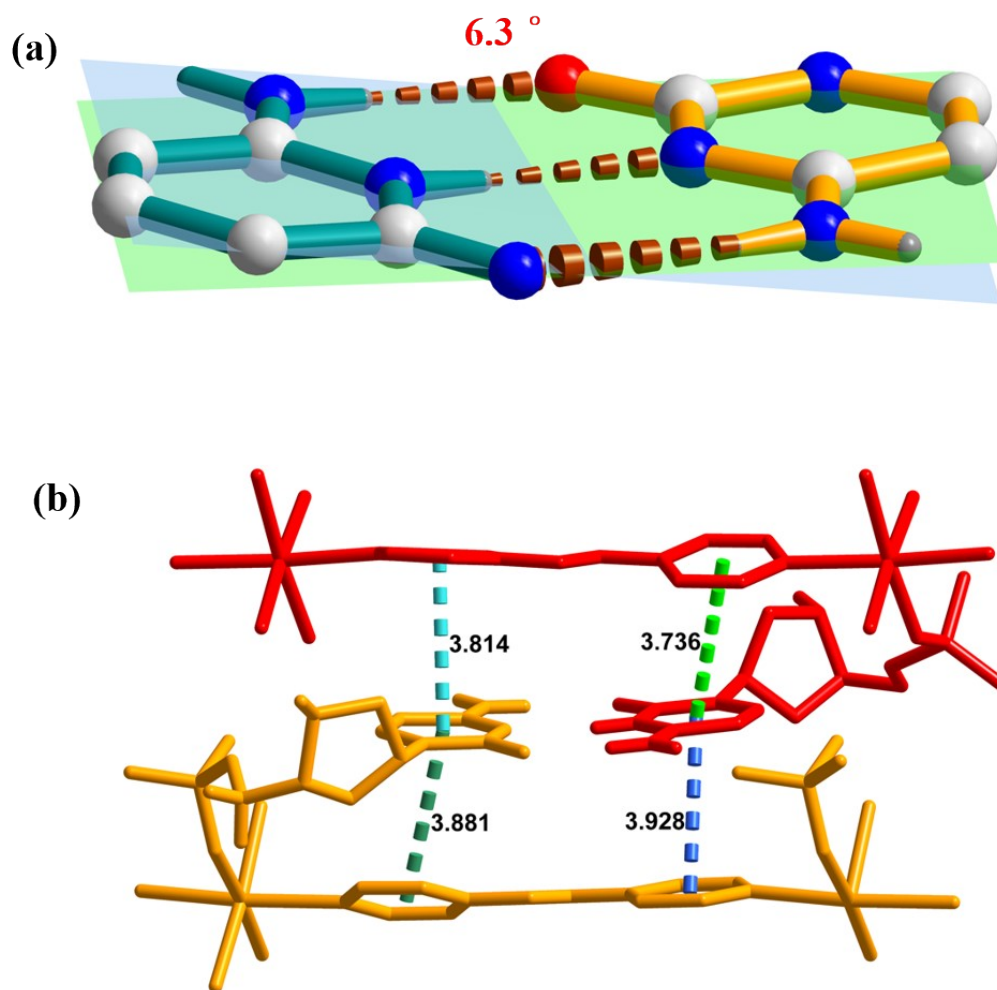
Figure S9. The dihedral angle of the plane formed by the methylene and pyridine-ring in bpa ligand complex **2**.
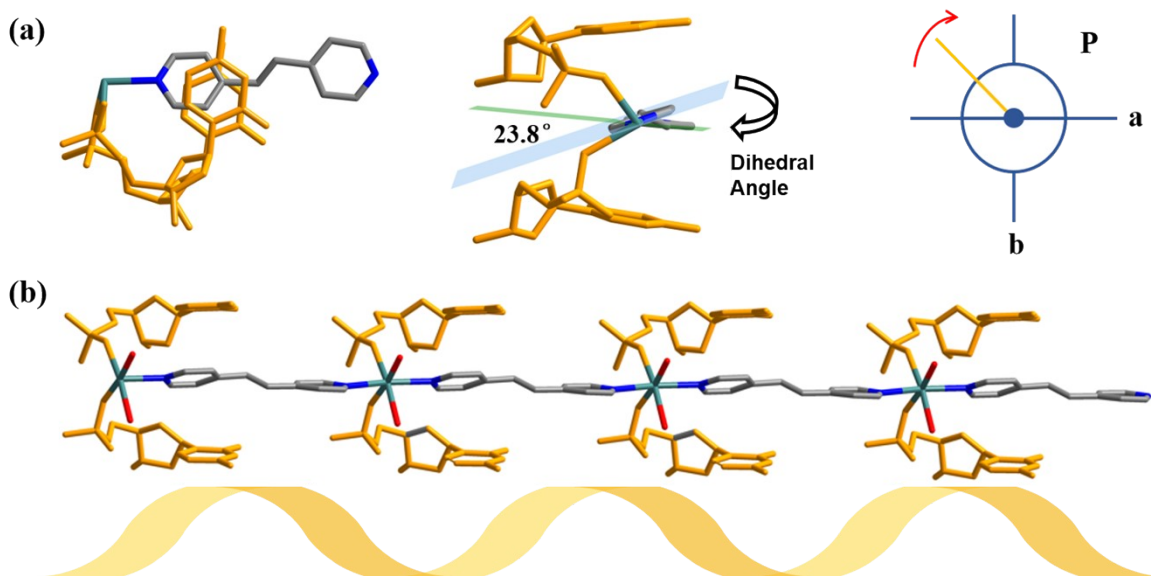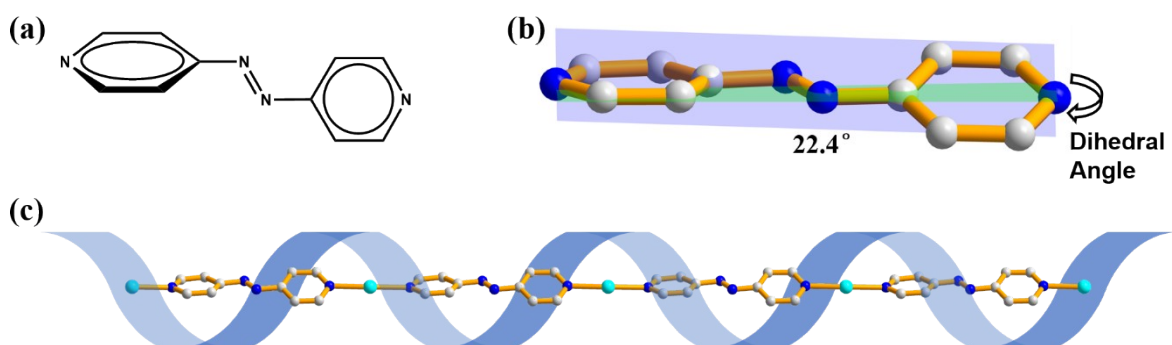

Figure S10. (a) The dihedral angle of bpa in complex **2** the clockwise-orientated nucleotide ligand inducing *P*-supramolecular chirality. (c) EAC chirality in complex **2** generated from M-L coordination and inducement of chiral nucleotides.

4. Supporting information of Complex 3
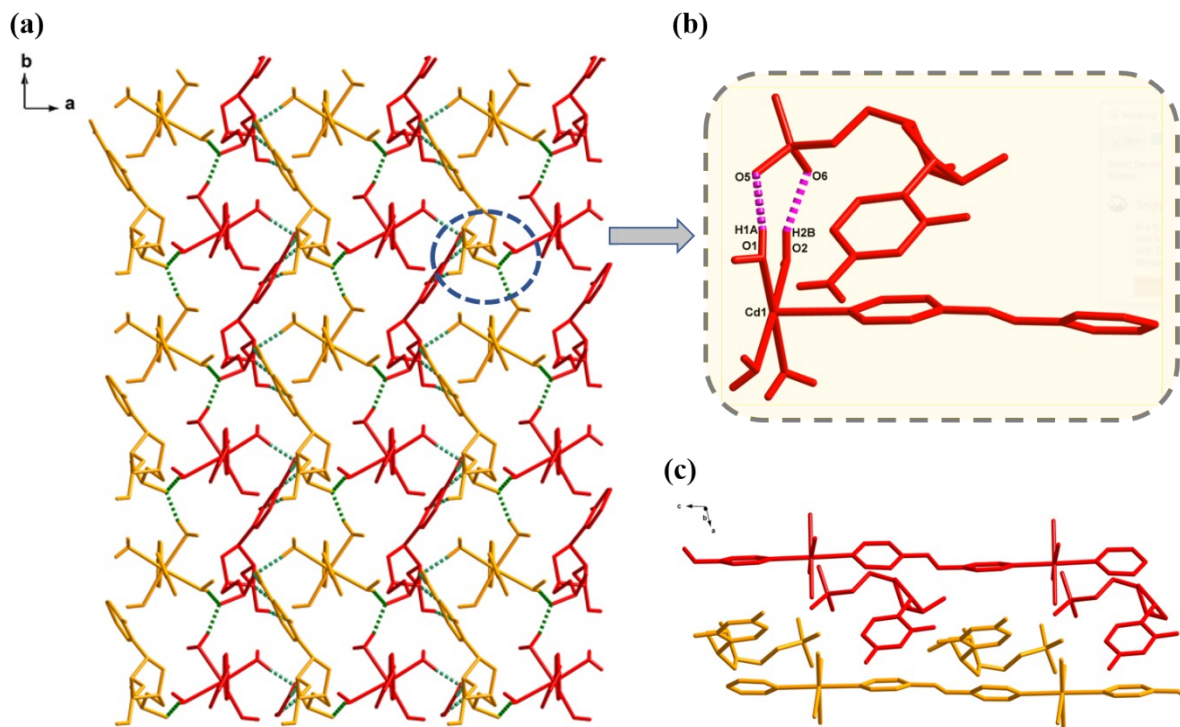
Figure S11. (a) and (b) The 3D supramolecular structure formed by hydrogen bonds between the coordinated water molecules and accepter atoms from the CMP^{2-} ligands.
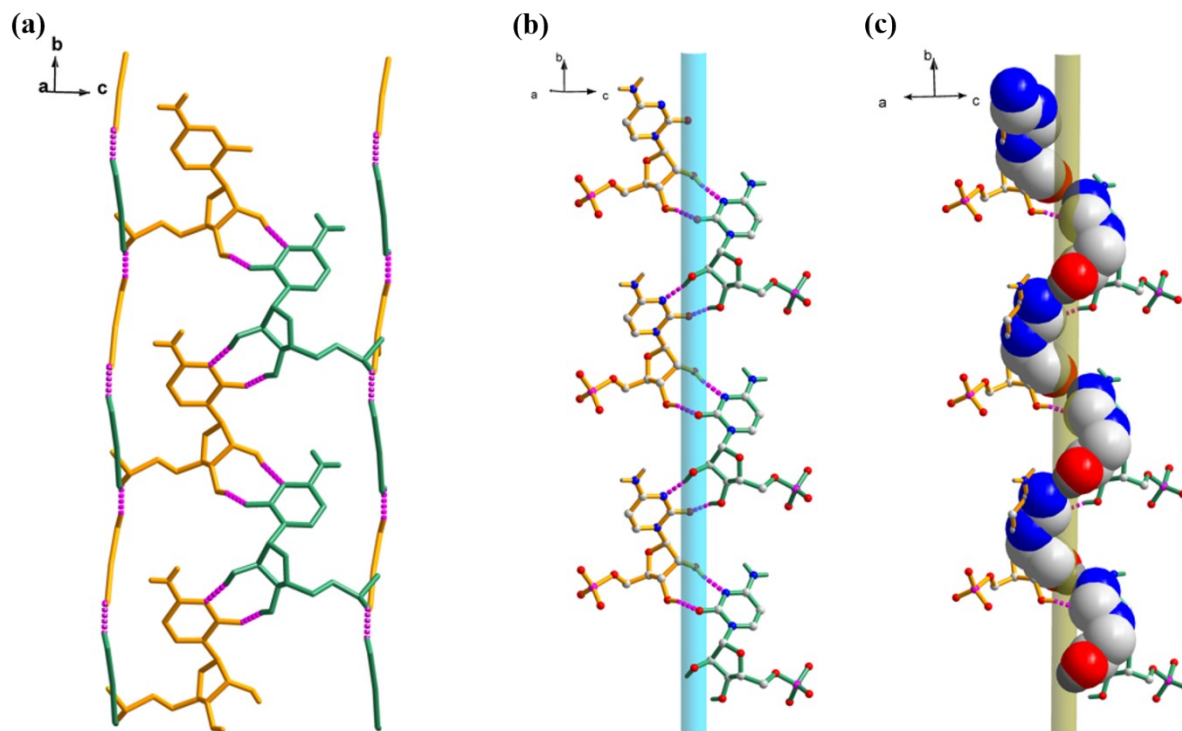
Figure S12. (a) 3D framework formed by nucleotide ligands connecting by hydrogen bonding. (b) and (c) Supramolecular helix formed by hydrogen bonding between sugar-nucleobase interaction of **3**, azpy ligands are omitted for clarity.
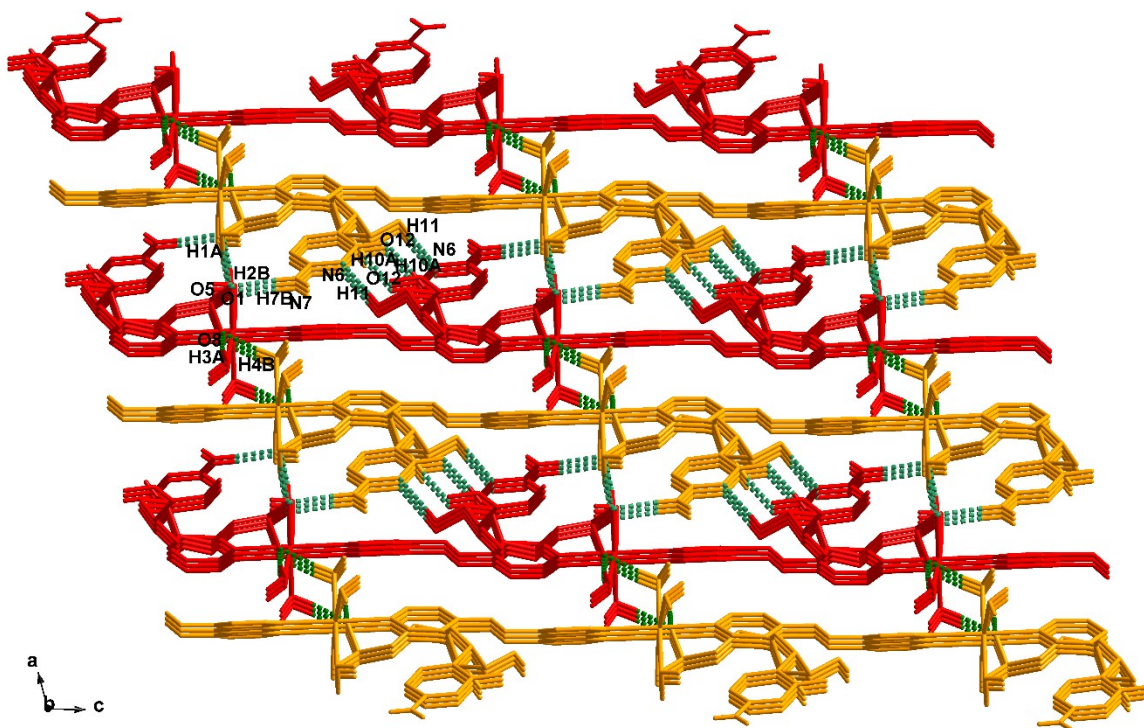
Figure S13. 3D supramolecular framework based on hydrogen bonding viewed down from the *b*-axis. The hydrogen bonding of the sugar-ring hydroxyl group to the carbonyl oxygen atom and the imine nitrogen atom of the base (green dashed lines, (O11–H11···N6), 0.82 Å, 2.05 Å, 168°; O10–H10A···O12, 0.82 Å, 1.78 Å, 164°), hydrogen bond between phosphate oxygen and pyrimidine base as well as the coordination water and the phosphate oxygen atom (O1–H1A···O5, 0.85 Å, 1.81 Å, 171°; O2-H2B···O6, 0.85 Å, 1.88 Å, 159°).
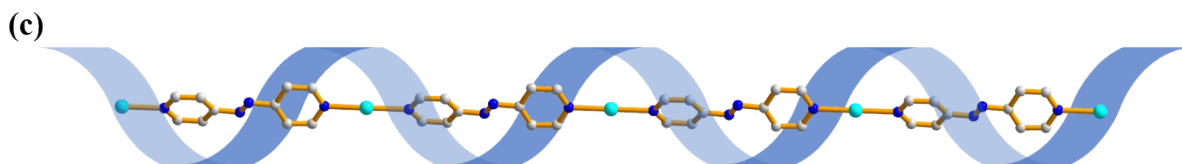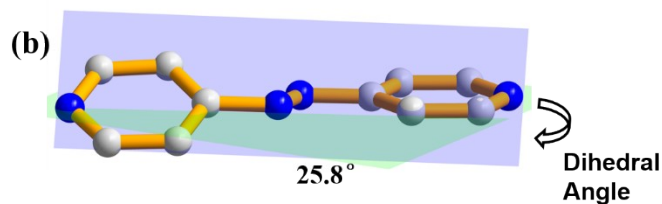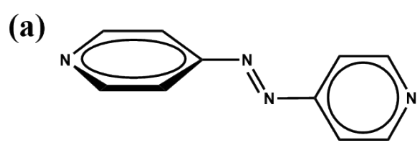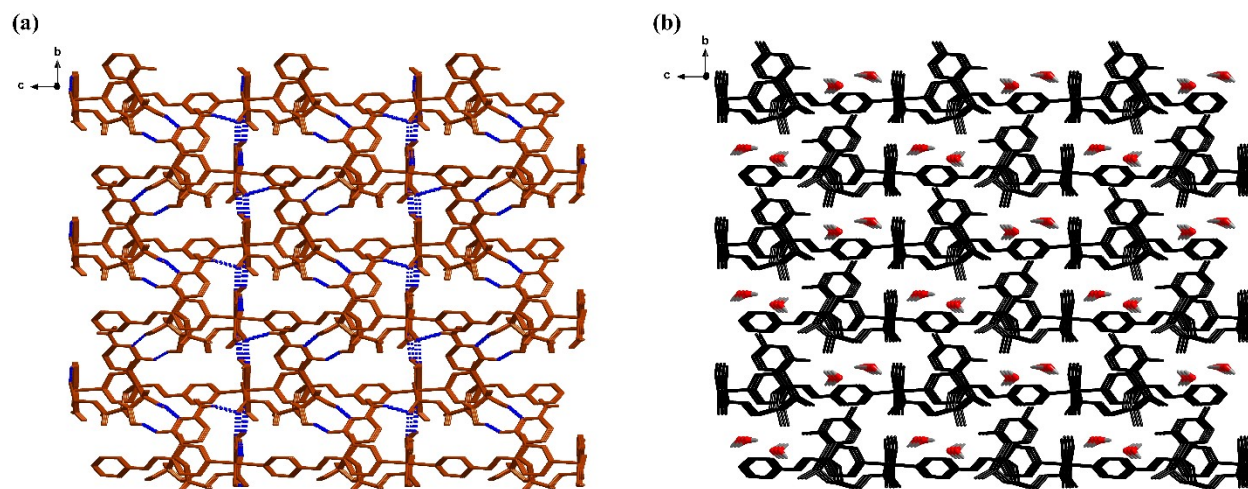
Figure S14. The dihedral angle of the plane formed by the methylene and pyridine ring in azpy ligand complex **3**.
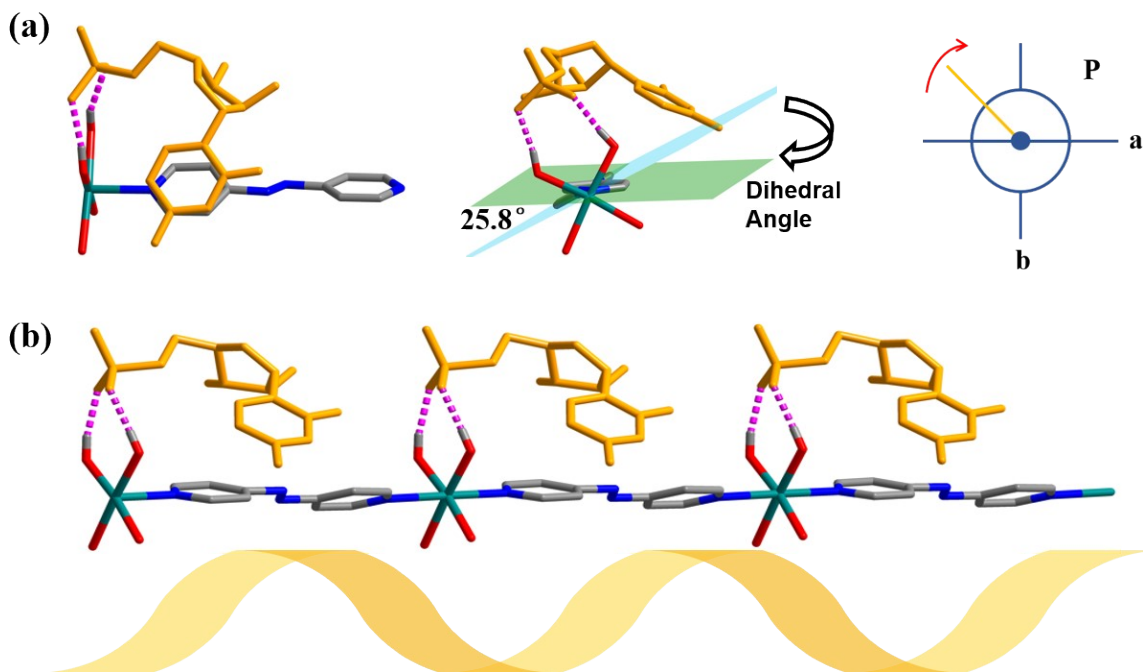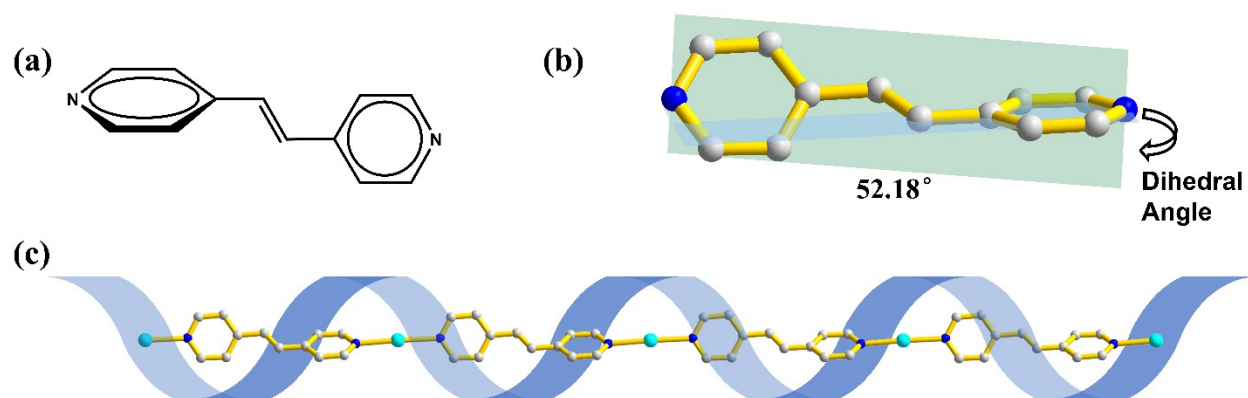

Figure S15. (a) The dihedral angle of azpy in complex **3** the clockwise-orientated nucleotide ligand inducing *P*-supramolecular chirality. (c) EAC chirality in complex **3** generated from M-L coordination and inducement of chiral nucleotide.

5. Supporting information of Complex 4

Figure S16. (a) i-motif angle in complex **4,** and complementary H-bonding between nucleobases. (b) the i-motif is further stabilized by π–π stacking interactions.

Figure S17. The dihedral angle of the plane formed by the methylene and pyridine ring in azpy ligand complex **4**.

(a)

(b)
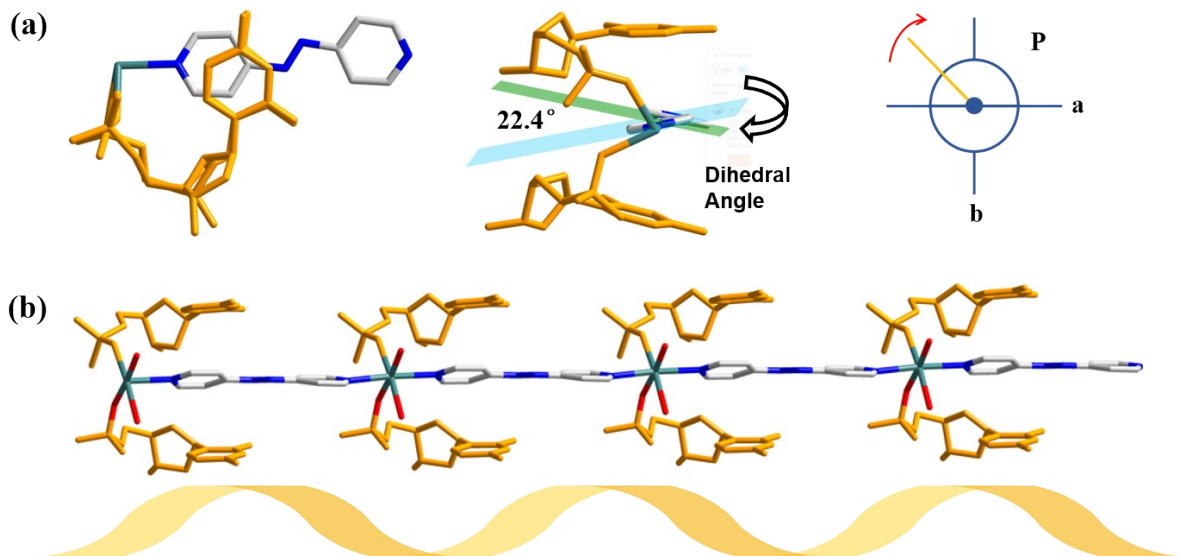
Figure S18. (a) The dihedral angle of azpy in complex **4** the clockwise-orientated nucleotide ligand inducing *P*-supramolecular chirality. (c) EAC chirality in complex **4** generated from M-L coordination and inducement of chiral nucleotides.

6. Supporting information of Complex 5

(a)

(b)

Figure S19. (a) 3D coordination network of complex **5** formed by hydrogen bonding between sugar-nucleobases viewed down from *a* axis. (b) Detail of the channels that are formed in the 3D polymeric structure of **5** that are filled with water molecules.

(a)

(b)

52.18°

Dihedral Angle

(c)

Figure S20. The dihedral angle of the plane formed by the methylene and pyridine ring in bpe ligand complex **5**.

(a)

52.18°

Dihedral Angle

M

a

b

(b)
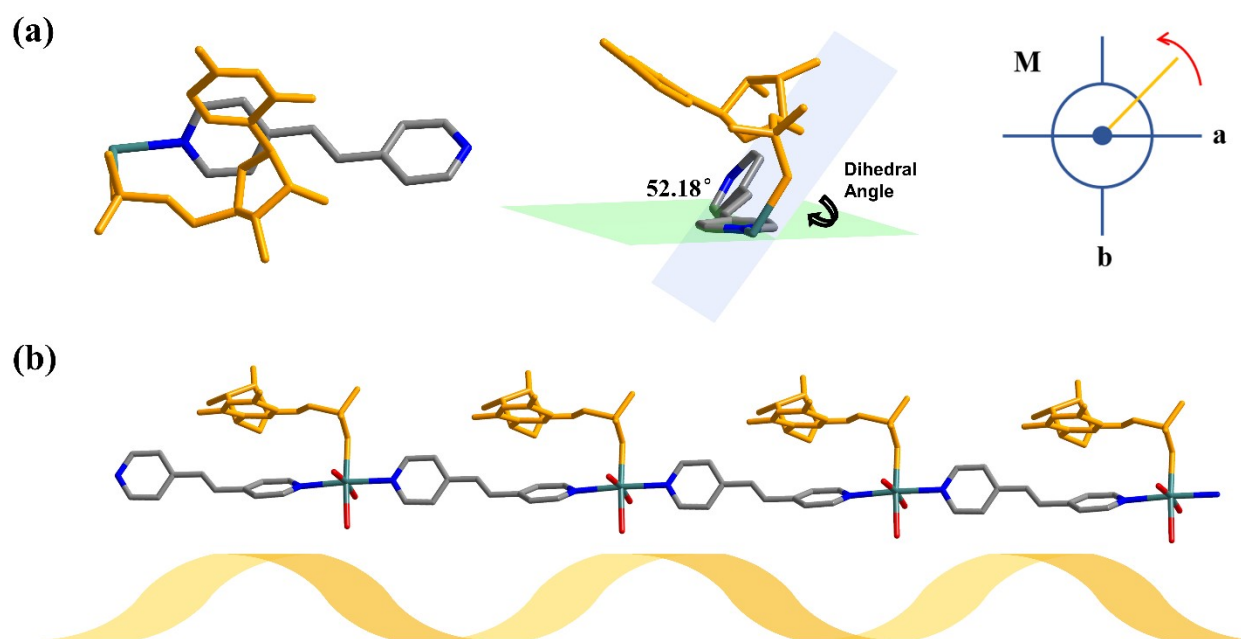
Figure S21. (a) The dihedral angle of bpa in complex **5**; the counter-clockwise orientated nucleotide ligand inducing *M*-supramolecular chirality. (c) EAC chirality in complex **5** generated from M-L coordination and inducement of chiral nucleotides.
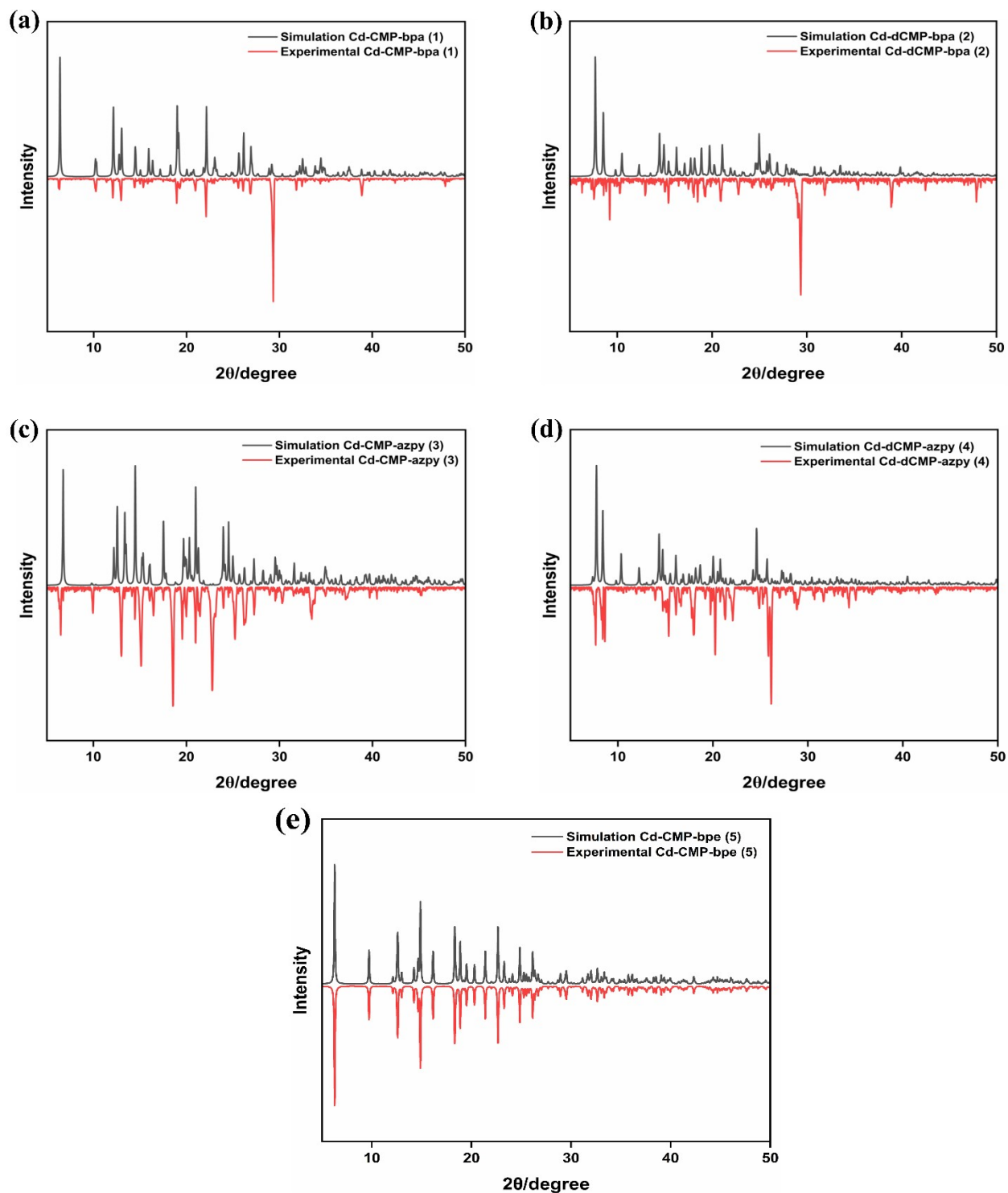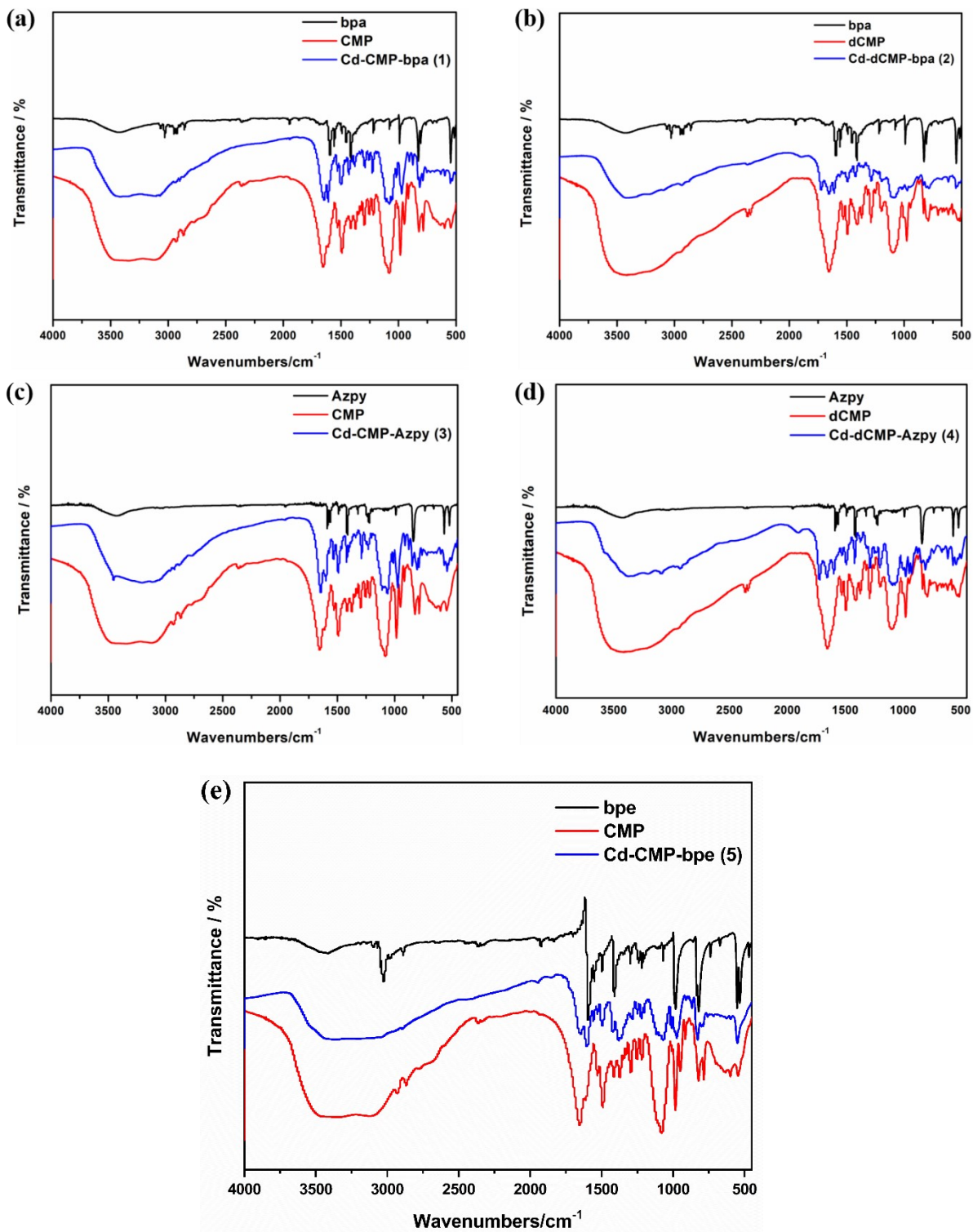
7. The PXRD Patterns of complexes 1-5

Figure S22. PXRD patterns show the comparison between the experimental values and calculated ones for (a) complex **1**, (b) complex **2**, (c) complex **3**, (d) complex **4**, and (e) complex **5**.

8. The FT-IR Spectra of complexes 1-5

Figure S23. IR spectra of (a) CMP, bpa, and complex **1**; (b) dCMP, bpa, and complex **2**; (c) CMP, azpy, and complex **3**;(d) dCMP, azpy, and complex **4**, CMP, bpe and complex **5**.
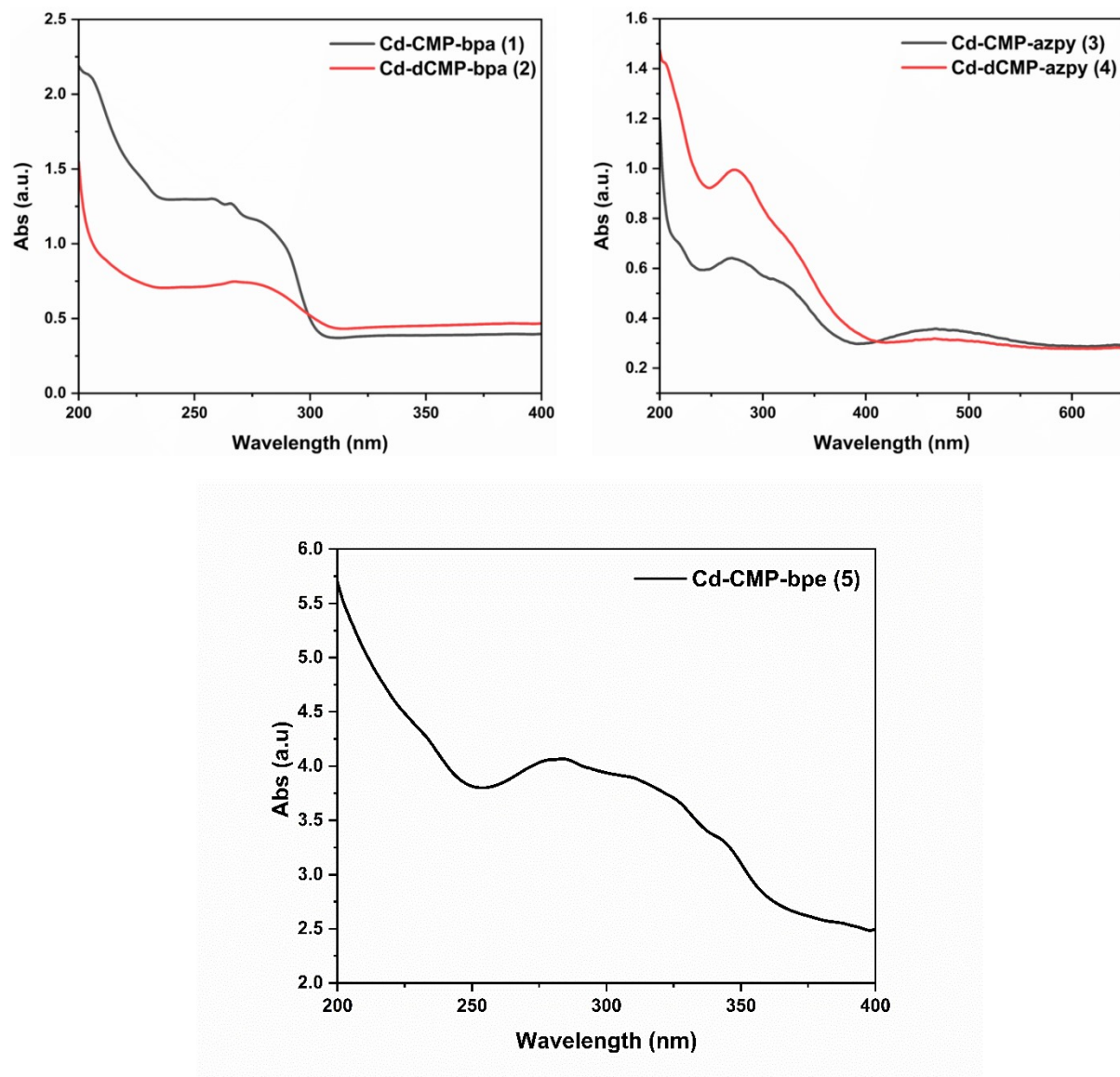
9. The Solution-State UV/*vis* Spectra of complexes 1-4
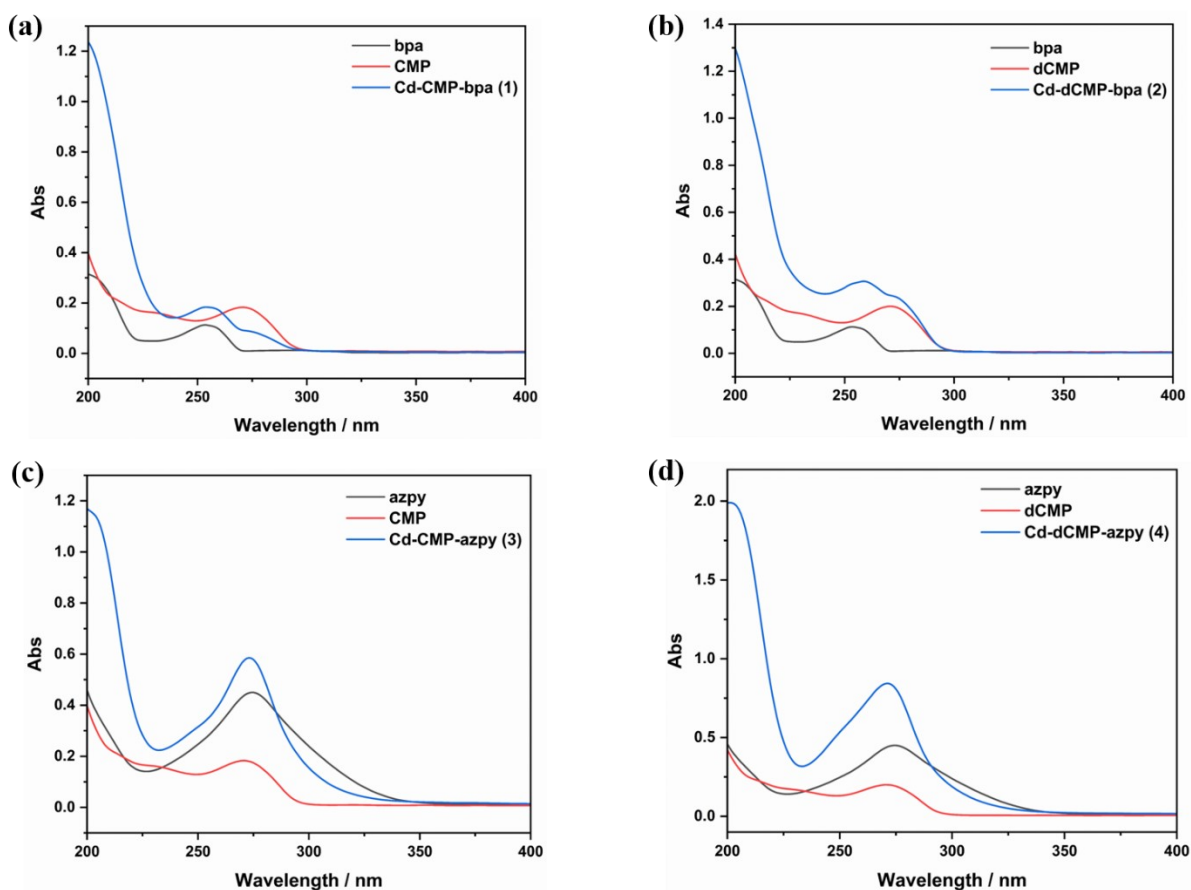
Figure S24. The solution-state UV/*vis* absorption spectra of (a) CMP, bpa, and complex **1**; (b) dCMP, bpa, and complex **2**;(c) CMP, azpy, and complex **3**; (d) dCMP, azpy, and complex **4**; (c) The relative absorption peaks. The spectra were obtained by measuring 2.5×10^{-5} mol·L^{-1} solution in a 1 cm cell.
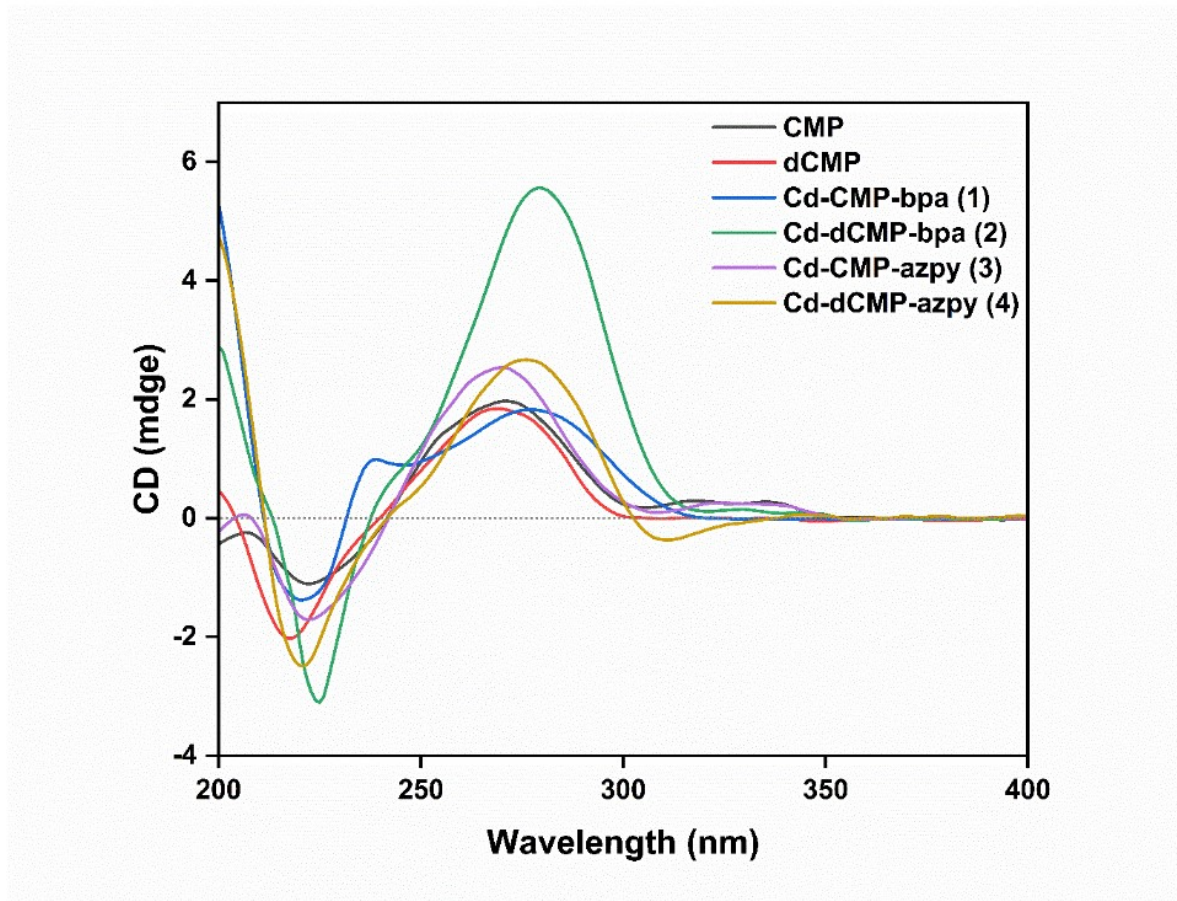
10. The Solid-State UV/*vis* Spectra of complexes 1-5


Figure S25. The solid-state UV/*vis* spectra of complexes **1**-**5** at room temperature. There exist d-d electron transitions in the region of 400-600 nm for complexes **3** and **4**.

11. The Solution-State CD spectra of CMP, dCMP, and complexes

Figure S26. The solution-state CD spectra of CMP, dCMP, and complexes at room temperature, the spectra were obtained by measuring 2.5×10^{-5} mol·L^{-1} water solution in a 1 cm cell.

12. The Thermo-Gravimetric Analysis of complexes 1-5
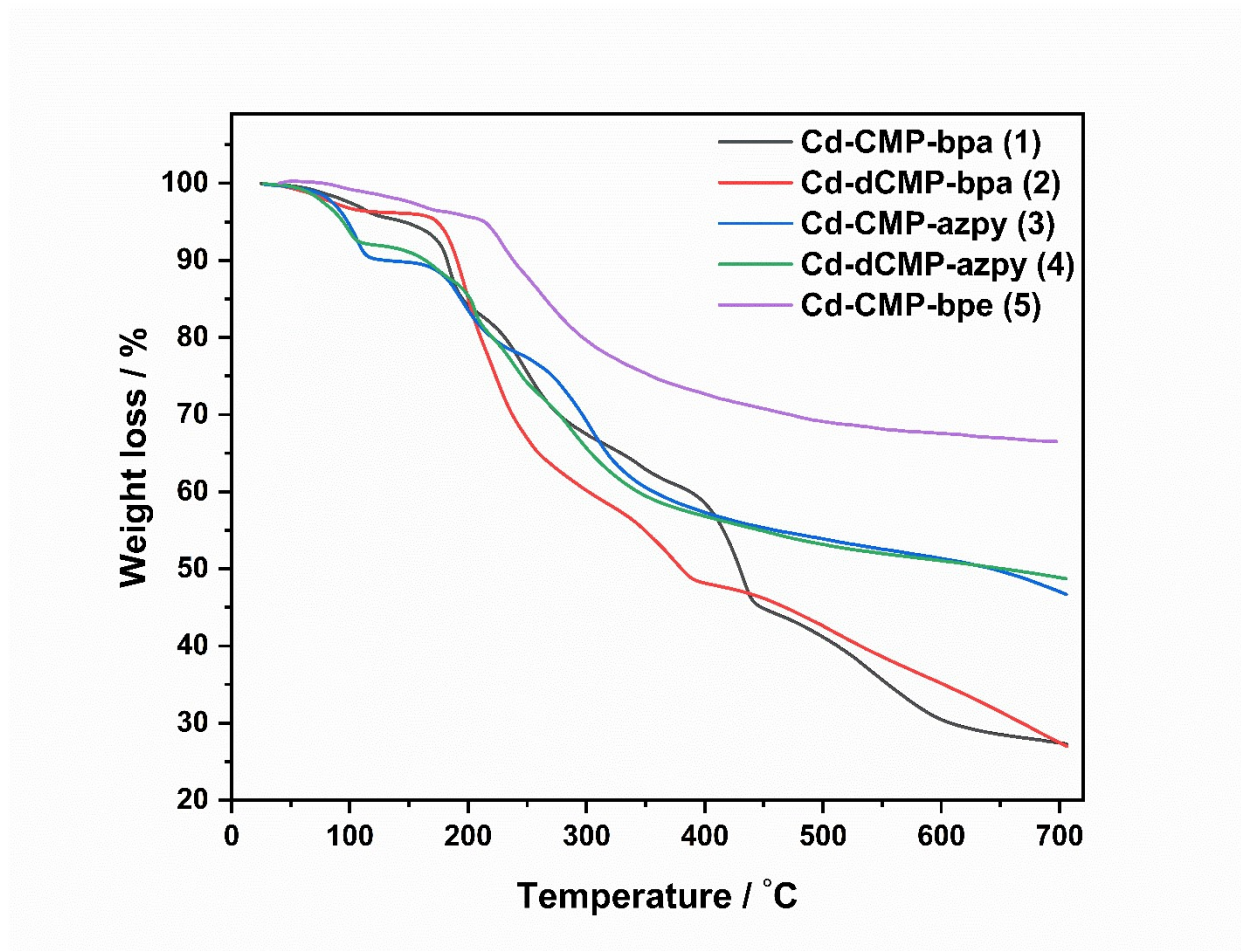
Figure S27. TG curves of complexes **1-5**.